X-Ray Diffraction Study of Hcp Metals

I. Line Broadening in Polycrystalline Cd Powder

N. C. Halder and S. H. Hunter *

Department of Physics, University of South Florida, Tampa, Florida 33620

(Z. Naturforsch. **29 a**, 1771–1777 [1974]; received August 15, 1974)

Powder Cd of 99.999% purity was prepared at room temperature (25 °C) and x-ray diffraction patterns were obtained using CuKα radiation with Ni-filter. The line broadening was analyzed after incorporating the appropriate correction factors. At room temperature Cd was found to have large particle size (653 A), small root mean square strain (.001), small deformation fault probability α(.003), and negligible growth fault probability β(0). Compared to other hcp metals which have been studied earlier and which have higher melting temperatures, metal Cd is much less affected by mechanical deformation at room temperature.

1. Introduction

X-ray diffraction technique is a valuable tool for examining the properties of polycrystalline materials. An analysis of the powder pattern peaks can determine the microstructure and the lattice properties of the material being examined [1–4]. The broadening of a peak is caused by faulting, by smallness of crystallite size, and by microstrains within these crystallites. A shift in the position of the peak maximum and an asymmetry can be due either to lattice parameter changes, or faulting, or residual stresses in the material. The degree of broadening can be determined by an analysis of the integral breadth or Fourier coefficients or variance of the peak, and the different causes can be separated [4]. These methods have been used to study the properties of many metals and alloys, particularly to investigate the effect of deformation due to mechanical forces [4–6]. The microstructure of deformed metals, polycrystalline films, and, more recently, chemically prepared powders such as polymers have been examined. Depending on the preparation and the prehistory, these materials may contain a high degree of faulting and internal stresses or may show little or no residual effects at room temperature [2]. Studies have been made [4] to understand the recovery of deformed materials with gradual annealing and pressure changes. Other studies [3] have compared the deformation effects in alloys with changing atomic concentration of one of the elements. Particle size, faulting, and strain of face centered cubic (fcc) and body centred cubic (bcc) materials have been extensively studied [4–6], but there are relatively few studies of hexagonal close packed (hcp) metals.

The purpose of this investigation is to study hcp Cd. We are interested in the study of this metal for several reasons: First of all, Cd is relatively soft and has a low melting temperature (321 °C) in contrast to the high melting temperature of Co (1495 °C) and Re (3167 °C) whose line broadening studies have been done earlier [3]. We would like to find out whether or not this low melting point metal has any line broadening due to faulting, strain, and particle size at the room temperature. Secondly, since the recrystallization temperature ($\frac{1}{2}\,T_m > 297$ °K), of Cd is very low any annealing studies at higher temperature is not undertaken. However, we expect the room temperature study will give us a considerable insight into the line broadening phenomena in the low melting point hcp metals; this kind of study is quite important and has not been reported before. Thirdly, solid state properties of Cd, such as, electronic and band structure properties are of considerable interest [7–9]. We shall be interested here in the study of microstructure of Cd that might affect the physical properties.

2. Experimental

Cd shots of purity 99.999% were obtained from Apache Chemicals. To make powder samples, the shots were filed at room temperature using small die-cutter files. It was assumed that in addition to producing a small size of the actual pieces of Cd, this filing would also cause the individual region of

* Present address: Department of Applied Physics, Stanford University, Stanford, California 94305.
Reprint requests to Prof. Dr. N. C. Halder, University of South Florida, Department of Physics, *U.S.A. Tampa/Florida 33620.*

crystallinity to be smaller, and would produce microstrains and faulting within those regions. Any rise in temperature during filing was avoided by changing files quite often and carrying out the process very slowly. The filings were then passed through 140 mesh sieve so that the powder size was approximately 0.105 mm diameter or smaller.

The powder patterns were recorded on a vertical Philips diffractometer with the Bragg-Brentano (flat sample) focusing condition. The x-ray source was a Philips XRG-2500 x-ray unit with copper radiation. The white radiation and Kβ components were eliminated by using a Ni β-filter. Only the Kα_1 and Kα_2 radiation remained, Kα_2 being half the intensity of Kα_1 line. The x-ray beam was passed through a 1° divergence slit and struck the flat sample before it was received through a receiving slit $.006^\circ$. A scintillation counter was used for detection of the diffracted beam.

First, the alignment of the x-ray instrument was checked by scanning the (110) and (321) peaks of a standard (well annealed) tungsten sample of lattice constant 3.1652 A. For each powder sample, individual peak was scanned at a speed of $1/8^\circ$ per minute in two theta across from low angle to high angle side. Because of the significance of the peak tails, sufficient care was taken to recover the background levels. In the analysis, two orders of the same reflection were needed to determine the strain. However, three types of reflections were needed to determine the two fault probabilities. In all, six diffraction peaks were chosen for the line profile analysis in the present investigation. The (002) and (004) peaks were a suitable pair for the strain calculation. For the study of faulting, the strong peaks, such as, (100), (101), (102) and (103) were selected.

Most of the calculations involved in our study were carried out with a computer program [10] DIFFN which we modified to suit our need for an hcp metal. It is a versatile program with options for the proper analysis of data from either a standard sample or a deformed sample, for use with either a β-filter or a monochromator crystal, for any x-ray wavelength, and for comparison of two peaks in a calculation of strain and particle size. The program was run on an IBM 360/65 computer with a Cal-Comp plotter.

3. Theoretical Considerations

A) Separation of Particle Size, Faulting and Strain

Since the strain broadening depends on the order of the reflection, and since broadening from particle size and faulting is independent of the order, these terms can be separated using the peak profiles of two or more orders of a reflection. Warren [11] expressed the Fourier coefficients as a product of the two terms:

$$A(L) = A^{\mathrm{D}}(L)\, A^{\mathrm{PF}}(L)\,, \tag{3.1}$$

where $L = n\, d_{hkl}$, is a distance in the crystal normal to the reflecting plane $h\,k\,l$ of interplanar spacing d_{hkl} and order n. The Fourier Coefficients $A(L)$ are obtained from the scattered intensity $I(s)$ of the pure diffraction profile:

$$A(L) = \int_{-\infty}^{\infty} I(s)\, \exp\{2\,\pi\, i\, L(s - s_0)\}\, \mathrm{d}s\,,$$

where $s = 2 \sin\theta/\lambda$, λ is the wavelength used and s_0 corresponds to the peak maximum θ_0.

The distortion or strain term $A^{\mathrm{D}}(L)$ is Gaussian in L for small L and strain ε_L:

$$\begin{aligned} A^{\mathrm{D}}(L) &= \exp\{[-2\,\pi^2\, L^2/d^2_{hkl}]\,(\langle \varepsilon_L{}^2\rangle - \langle \varepsilon_L\rangle^2)\} \\ &\cong 1 - [2\,\pi^2\, L^2/d^2_{hkl}]\,(\langle \varepsilon_L{}^2\rangle - \langle \varepsilon_L\rangle^2)\,, \end{aligned} \tag{3.2}$$

where $(\langle \varepsilon^2{}_L\rangle - \langle \varepsilon_L\rangle^2)$ is the standard deviation of the strain which is given by $\varepsilon_L = \Delta L/L$. The term $A^{\mathrm{PF}}(L)$ due to particle size and faulting, can be approximated for small L:

$$A^{\mathrm{PF}}(L) \cong 1 - L/D_{\mathrm{eff}}\,, \tag{3.3}$$

where D_{eff} is the effective domain size normal to the reflecting planes, due to both true particle size and to faulting. If two orders of a reflection are available, then both $A^{\mathrm{PF}}(L)$ and $(\langle \varepsilon^2{}_L\rangle - \langle \varepsilon_L\rangle^2)$ can be separated using

$$\begin{aligned} \ln A(L) &\cong \ln A^{\mathrm{PF}}(L) \\ &\quad - [2\,\pi^2\, L^2/d^2_{hkl}]\,(\langle \varepsilon_L{}^2\rangle - \langle \varepsilon_L\rangle^2)\,. \end{aligned} \tag{3.4}$$

These values can be obtained numerically or found graphically from the slope and intercept of a plot of $\ln A(L)$ versus $1/d_{hkl}$.

The integral breadth can be calculated from the Fourier coefficients

$$b(s) = \left[\int_{-\infty}^{\infty} A(L)\, \mathrm{d}L\right]^{-1}. \tag{3.5}$$

Thus the broadening due to particle size and faulting is given by

$$b^{\mathrm{PF}}(s) = \left[\int_{-\infty}^{\infty} A^{\mathrm{PF}}(L)\, \mathrm{d}L\right]^{-1} = 1/D_{\mathrm{I}}{}^{\mathrm{PF}}\,, \tag{3.6}$$

where $D_{\mathrm{I}}{}^{\mathrm{PF}}$ is the integral breadth particle size composed of the true particle size $D_{\mathrm{I}}{}^{\mathrm{P}}$ and the fault

particle size D_1^F. Similarly, the strain integral breadth is given by (for Gaussian strain distribution)

$$b^\varepsilon(s) = [\int_{-\infty}^{\infty} A^D(L)\,dL]^{-1} \cong 2\,\varepsilon_1 S_0 = 2\,\varepsilon_1/d_{hkl}, \quad (3.7)$$

where ε_1 is strain, assumed to be independent of L. Several methods have been suggested for the separation of strain and particle size in the integral breadth measurements [12–15], but we shall discuss the one which is believed to be the most practical. Schoening [15] showed that the line profile is best described by a convolution of a Cauchy particle size function with a Gaussian strain function. Thus, the integral breadth is given by

$$b(s) = b^\varepsilon \exp\{-(b^P/\sqrt{\pi}\,b^\varepsilon)^2\}/[1-\mathrm{erf}\,(b^P/\sqrt{\pi}\,b^\varepsilon)], \quad (3.8)$$

where

$$\mathrm{erf}(b^P/\sqrt{\pi}\,b^\varepsilon) = \frac{2}{\sqrt{\pi}} \int_0^{b^P/\sqrt{\pi}b^\varepsilon} \exp\{-t^2\}\,dt.$$

We have demonstrated earlier [12] that, to a good approximation, the above equation can be reduced to a convenient and useful form,

$$b^{PF}(s)/b(s) = 1 - [b^\varepsilon(s)/b(s)]^2. \quad (3.9)$$

We will employ this equation to obtain D_1^{PF} and ε_1 from two or more orders of a reflection.

B) Separation of Particle Size and Faulting in Hcp Powders

The effective particle size D_{eff} can be found by plotting the particle size faulting coefficients $A^{PF}(L)$ versus L. The slope of this curve extrapolated to $L=0$, gives the effective particle (also called domain) size,

$$-(dA^{PF}/dL)_{L=0} = 1/D_{eff}. \quad (3.10)$$

In hcp crystals, the (002) planes form close packed layers with the normal stacking sequence ABABABAB. A growth stacking fault occurs when the stacking changes from AB to BC as in the sequence ABABCBCB. A deformation stacking fault with the sequence ABABCACA introduces a small range with fcc stacking order. Warren [4] assumed that the stacking faults occur independently on these (002) planes and showed that faulting produces an effective domain size D_{hkl}^F for $(h\,k\,l)$ planes in three different ways, which can be placed in three different groups. In terms of the Fourier coefficients, these equations are:

Group one, $h-k=3N$ with $l=0$,

$$-(dA^{PF}/dL)_{L=0} = 1/\overline{D}. \quad (3.11)$$

Group two, $h-k=3N\pm1$ with l even,

$$-(dA^{PF}/dL)_{L=0} = 1/\overline{D} + (|l|\,d/c^2)\,(3\alpha+3\beta). \quad (3.12)$$

Group three, $h-k=3N\pm1$ with l odd,

$$-(dA^{PF}/dL)_{L=0} = 1/\overline{D} + (|l|\,d/c^2)\,(3\alpha+\beta). \quad (3.13)$$

For the two groups of fault affected peaks, the integral breadth can also be used:

For $h-k=3N\pm1$ with l even

$$b^{PF}(s) = (|l|\,d/2\,c^2)\,(3\alpha+3\beta). \quad (3.14)$$

For $h-k=3N\pm1$ with l odd

$$b^{PF}(s) = (|l|\,d/2\,c^2)\,(3\alpha+\beta), \quad (3.15)$$

where the symbols α = deformation fault probability, β = growth fault probability, c = lattice parameter along c-axis, and d = interplanar spacing. We shall utilize the above theory in the next section.

4. Results of the Analysis

In order to perform the Stokes correction for instrumental broadening, a suitable standard sample must be chosen. A standard sample must have very large particle size, practically no strain, and no faulting so that it has very sharp peaks defined only by the geometric condition of the experiment. This means that the Fourier coefficients of the standard sample should be larger than those of the experimental samples of our interest.

To remove the instrumental broadening, we prepared three annealed samples, much above the recrystallization temperature. All these samples were carefully examined for their consistency for line broadening effect. When there was no variation from one sample to another, except of course that due to statistical fluctuations, the average values of their Fourier coefficients were considered for the standard sample.

The strain and particle size coefficients were obtained from the Stokes corrected Fourier coefficients of the (002) and (004) peaks, as shown in Fig-

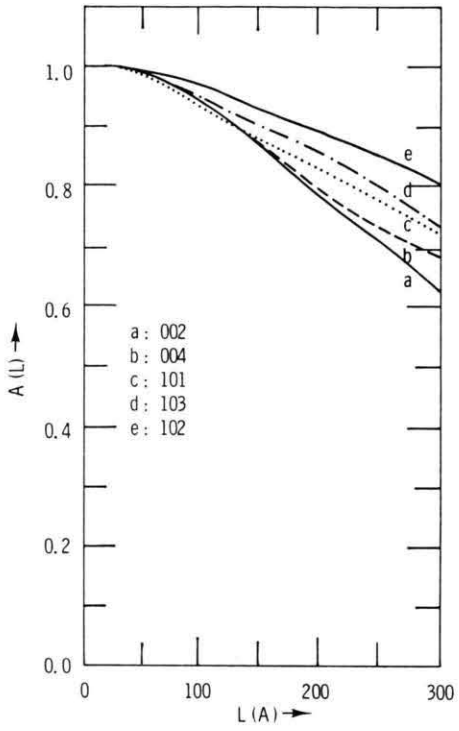

Fig. 1. Stokes corrected Fourier coefficients.

ure 1. Since these peaks are unaffected by faulting, we can calculate directly the particle size coefficients $A^{P}(L)$ and the strain coefficients $A^{D}(L)$. The coefficients $A^{P}(L)$ are shown in Figure 2. The true particle size $\overline{D}$ is found from the slope of the linear portion of the curve. This is shown in Table 1. The

Tab. 1. Particle size and strain by Fourier coefficients method.

$\langle \varepsilon^2_L \rangle^{1/2}$	$\overline{D}$ (002,004)
.0010	653 A

strain and particle size were also calculated from the integral breadth of the (002) and (004) peaks. The integral breadth particle size D_I is only slightly larger than the Fourier analysis particle size $\overline{D}$. The integral breadth strain ε_I is about half the value of the rms strain of the Fourier analysis. As is clear, the rms strain is quite small and has negligible effect on the line broadening. The particle size is rather large, but still within the limit of validity of the Warren-Averbach [11] method (less than 5000 A). For the fault broadened reflections, since the dominating term is expected to be that due to faulting, we may neglect effect of the large particle size and small rms strain in these reflections and obtain at once the

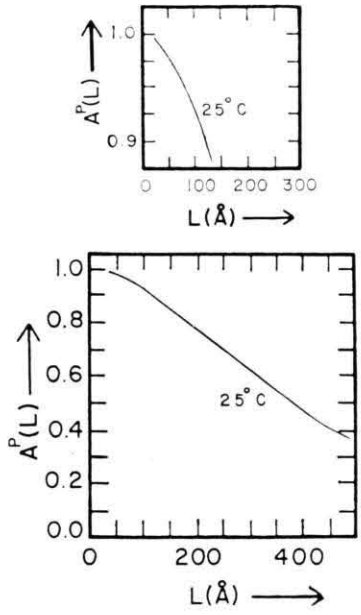

Fig. 2. Plot of the particle size coefficients $A^{P}(L)$.

fault probabilities. The faulting terms $(3\alpha+3\beta)$ and $(3\alpha+\beta)$ were thus determined. For the Fourier coefficient method we can obtain the fault particle size D^{F} directly from the slope of the $A(L)$ versus L curve. In this way, the two faulting terms were calculated for peaks (101), (102) and (103). These values are listed in Table 2. We find that the values calculated from the integral breadth are always

Tab. 2. Deformation (α) and growth (β) fault probabilities by Fourier coefficients (FC) and integral breadth (IB).

$(h\,k\,l)$	Terms	FC	IB
102	$3\alpha+3\beta$	.00610	.0199
101	$3\alpha+\beta$	.01494	.0340
103	$3\alpha+\beta$	.00630	.0179
Average α $\beta=0$		.00304	.0080

larger than those calculated from the Fourier coefficients. From a general trend of these values, it seems that the growth fault probability β is either very small or zero, and that the deformation fault probability α is on the order of $.003 \sim .002$ for the Fourier coefficients, but $.008 \sim .007$ for the integral breadth. At this point we can note that Cd appears to have been very little affected by mechanical deformations compared to other hcp metals studied earlier [16–19].

Lele [20] has calculated theoretically the effect of layer faults in hcp crystals. A layer fault consists of a spacing fault (change in interplanar spacing) in conjunction with a stacking fault (change in the stacking order). Changes in the interlayer distance are unlikely in close packed metals due to the non-directional nature of the bonding. However, Lele [20] suggested that in the region of a stacking fault the change in structure may allow a spacing fault also. Assuming an infinite crystal size, random fault distribution, and extension of faults over the entire domain, Lele [20] found that the integral breadth and intensity would not be affected by the layer fault. However, peak shifts would occur which are equivalent to a change in the lattice parameter c to $c(1+\alpha'\delta)$, where α' is the layer fault probability. The reflections with $h-k=3N$ are shifted twice as much and in the opposite direction as the reflections with $h-k=3N\pm1$. Therefore,

for $h-k=3N$, $\delta \ll 1$

$$\Delta(2\theta^0) = -\frac{720}{\pi}\frac{l^2 d^2}{c^2}(\tan\theta)\,\gamma\,\delta\,, \qquad (4.1)$$

where

$$\gamma = \alpha'(1+\alpha') \cong \alpha' \text{ for small } \alpha'\,. \qquad (4.2)$$

For $h-k=3N\pm1$, $\delta \ll 1$

$$\Delta(2\theta^0) = \frac{360}{\pi}\frac{l^2 d^2}{c^2}(\tan\theta)\,\gamma\,\delta\,. \qquad (4.3)$$

In the above, reflections with $l=0$ should not be shifted. As shown in Fig. 3, we did observe a small change in the lattice parameter c compared to the crystalline value. In the sample prepared at room temperature, this would correspond to a value of $\alpha'\delta = .00038$. We compared the position of the peak maximum for each peak with the theoretical value calculated with the solid state lattice parameters. The observed peak shifts $\Delta(2\theta)^0$ are listed in Table 3. An examination of these data does not reveal a peak shift which is in opposite directions

Tab. 3. Peak shifts relative to solid crystalline value.
Peak Shift $= \Delta(2\theta^\circ) = 2\theta^\circ(\text{obs}) - 2\theta^\circ(\text{theo})$

(002)	(100)	(101)	(102)	(103)	(004)
−.15	−.17	−.15	−.16	−.12	−.10

for (002) and (101) peaks, not even when measured relative to the (100) peak which should remain unshifted. Thus, although Cd shows a small

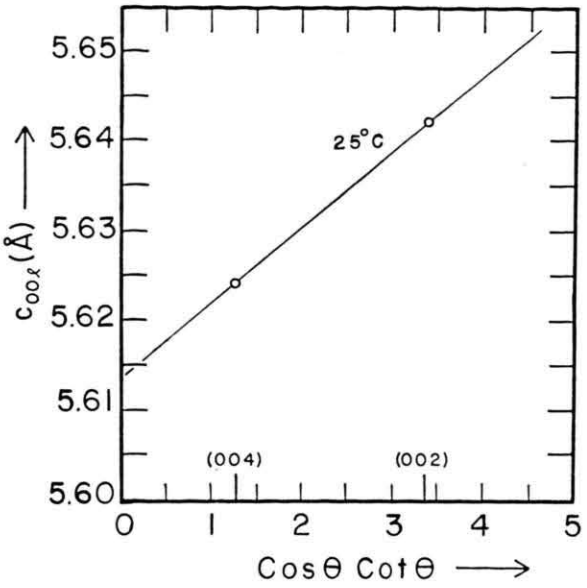

Fig. 3. Plot of the lattice parameter versus function $\cos\theta\cot\theta$.

lattice parameter change, there are no accompanying peak shifts in the manner predicted by Lele [20] for layer faults in hcp metals.

5. Discussions and Conclusions

Fewer x-ray line broadening studies have been made for hcp metals than for fcc and bcc. Among hcp metals, Co has been very extensively studied [17, 18, 21]. Mitra and Halder [18] examined the effect of annealing temperature on particle size, strain and the fault probabilities α and β. Particle size and strain were both larger when calculated using the integral breadth. However, the fault probability was larger when calculated using the Fourier coefficients. It should be noted that these methods actually measure different quantities. The Fourier analysis measures the average thickness of the coherently diffracting domains perpendicular to the (hkl) plane, whereas the integral breadth method measures the cube root of the average volume of these domains.

The x-ray diffraction peaks for Cd were not particularly broad. The Fourier coefficients were larger for Cd than for other hcp metals whose line broadening analysis have been carried out. The change in lattice parameter is rather small (see Table 4). The particle size in our samples was relatively large,

rms strain as well as the fault probabilities were small. As mentioned earlier, the overall effect of mechanical deformation in Cd at room temperature is much less than that noted in Re [16], Co [17, 18], and Mg [19].

Table 4. Lattice parameters.

Sample	a(A)	c(A)
Powder	2.9922	5.6132
Bulk	2.9787	5.6170

Studies of Zr [22] and Mg [23] have indicated no faulting. Mitra and Misra [19] separated strain and particle size in Mg using the single reflection method [24]. They found some anisotropy in the particle size, but had not considered faulting. A study on Re [16] also showed smaller particle size and rms strain with Fourier coefficients than integral breadth measurements, but the fault probability β was nearly the same for both the methods, assuming $\alpha = 0$. There are also some reports about the study of hcp alloys [25–27].

Lele et al. [23] suggested that the extrinsic stacking fault with the sequence ABABCABA would symmetrically broaden only the reflections with $h - k = 3N \pm 1$ and l odd, but would not cause any peak shift. A gradual introduction of such extrinsic faults in an hcp structure would eventually convert it to a double hexagonal close packed structure, but no example of such a structure transition in a metal is known. Mitra and Misra [19] calculated the temperature diffuse scattering (TDS) contribution to the diffraction pattern of Mg. Assuming a spherical first Brilliouin zone and only one phonon scattering, they found that the TDS peaks occurred at the same positions as the Bragg peaks and contributed appreciably to the tails of the diffraction peaks. The position of layer faults have been considered by Lele [20] for hcp crystals. He found no change in the integrated intensity and broadening, but predicted a peak shift for the reflections with $h - k = 3N$. However, this peak shift was twice as much and in the opposite direction as for the peaks with $h - k = 3N \pm 1$.

In conclusion, we can now summarize the important results of Cd obtained in the present investigation. While Co and Re have high melting temperatures, Cd has comparatively low melting temperature. Both Co and Re have smaller particle size than Cd. Re has negligible rms strain, no deformation fault probability, and a growth fault probability about .010. Likewise, Co at room temperature has small rms strain, a deformation fault probability about .02, and growth fault probability .05. Contrasting to these results, Cd has small rms strain, small deformation fault probability and no growth fault probability. These differences for Cd can be related to the lower melting temperature and higher temperature of study compared to the recrystallization temperature. Cd could, perhaps, show more faulting and rms strain at lower temperature (liquid nitrogen). Wagner [28] has studied a number of metals (fcc), Ag, Al, Cu, α-brass at liquid nitrogen temperature and found more faulting, rms strain and smaller particle size at lower temperature. Al has lower melting point and higher stacking fault energy than Ag. Furthermore, Al showed larger particle size, approximately the same rms strain, but no faulting even at low temperatures. Therefore, it seems that, although Cd does respond to mechanical deformation at room temperature it could be enhanced probably at low temperature. Consequently, it will be quite useful and important to study this metal in the region of liquid nitrogen temperature and follow up the annealing effect to room temperature.

[1] G. B. Greenough, Prog. Metal Phys. **3**, 176 [1952].
[2] D. M. Vasil'ev and B. I. Smirnov, Soviet Phys. Uspekhi **4**, 226 [1961].
[3] C. N. J. Wagner, Local Atomic Arrangements Studied by X-ray Diffraction, Gordon and Breach, Science Publishers, New York 1965.
[4] B. E. Warren, Prog. Metal Phys. **8**, 147 [1958].
[5] E. N. Aqua and C. N. J. Wagner, Phil. Mag. **9**, 565 [1964].
[6] C. N. J. Wagner and E. N. Aqua, Adv. X-ray Analysis **7**, 46 [1964].
[7] P. Jena, Ph. D. Thesis, University of California Riverside 1970.
[8] R. V. Kasowski and L. M. Falicov, Phys. Rev. Lett. **22**, 1001 [1969]; R. V. Kasowski, Phys. Rev. **187**, 891 [1969].
[9] P. Jena and N. C. Halder, Phys. Rev. Lett. **26**, 1025 [1971].
[10] C. N. J. Wagner, Technical Report No. 13, Office of the Naval Research, Yale Univ., New Haven, Conn., April, 1966.
[11] B. E. Warren and B. L. Averbach, J. Appl. Phys. **21**, 595 [1950].
[12] N. C. Halder and C. N. J. Wagner, Adv. X-ray Analysis **9**, 91 [1966].
[13] W. H. Hall, J. Inst. Met. **75**, 1127 [1949].

[14] G. V. Kurdyumov and L. I. Lysak, J. Tech. Phys. U.S.S.R. **17**, 993 [1947].
[15] F. R. L. Schoening, Acta Cryst. **18**, 975 [1965].
[16] C. N. J. Wagner and E. N. Aqua, J. Less-Common Metals **8**, 51 [1965].
[17] C. R. Houska and B. L. Averbach, Acta Cryst. **11**, 139 [1958]; C. R. Houska, B. L. Averbach, and M. Cohen, Acta Met. **8**, 81 [1960].
[18] G. B. Mitra and N. C. Halder, Acta Cryst. **17**, 817 [1964].
[19] G. B. Mitra and N. K. Misra, Acta Cryst. **22**, 454 [1967]; G. B. Mitra and N. K. Misra, Brit. J. Appl. Phys. (J. Phys. D) D **2**, 27 [1969].
[20] S. Lele, Acta Cryst. A **26**, 344 [1970].
[21] A. J. C. Wilson, Proc. Roy. Soc. A. **180**, 277 [1942]; T. R. Anantharaman and J. W. Christian, Acta Cryst. **9**, 479 [1956].
[22] J. H. Mogard and B. L. Averbach, Acta Met. **6**, 552 [1958].
[23] S. Lele, T. R. Anantharaman, and C. A. Johnson, Phys. Stat. Sol. **20**, 59 [1967]; S. Lele and T. R. Anantharaman, Phys. Stat. Sol. **5**, K 121 [1964].
[24] B. Y. Pines, Dokl. Akad. Nauk SSSR. **103**, 601 [1953].
[25] J. Spreadborough, Acta Cryst. **13**, 603 [1960].
[26] R. P. Stratton and W. J. Kitchingman, Brit. J. Appl. Phys. **16**, 1311 [1965].
[27] R. G. Davies and R. W. Cahn, Acta Met. **10**, 621 [1962].
[28] C. N. J. Wagner, Acta Met. **5**, 427 [1957]; **5**, 477 [1957].